

A Meshless Method for $2^{1/2}$ D Mold Filling Simulations Using Point Set Surfaces

K.C. ESTACIO¹, L.G. NONATO², Departamento de Matemática Aplicada e Estatística, ICMC, USP, 13560-970 São Carlos, SP, Brasil

N. MANGIAVACCHI³, Departamento de Engenharia Mecânica, FEN, UERJ, 20550-013 Rio de Janeiro, RJ, Brasil.

Abstract. In this work a novel meshless technique for mold filling simulation is presented. The governing equation for this kind of problem is named Hele-Shaw and it is derived applying some simplifications on the 3D conservation equations. This approach is also commonly called $2^{1/2}$ D, referring to limitations of the mold geometry to narrow and weakly curved channels. Since products manufactured by injection molding in real life, as for example buckets, automobiles bumpers and cell phone casings, are not expected to be planar, in this work the mold cavity is modeled by point set surfaces. Thus, no computational effort referring to either mesh generation or mesh maintenance is required for the numerical solution of the governing equations. The developed technique for simulating the free surface position, velocity and pressure distribution in the injection molding process using this $2^{1/2}$ D approach is presented and discussed. The details of our framework, which is based on Smoothed Particle Hydrodynamics Method and a Meshless Volume of Fluid Method is also presented.

1. Introduction

Injection molding is one of the most important industrial processes for the manufacturing of thin plastic products. Examples of such products are cassette tape boxes, children masks, and computer keyboards. In the production process, molten polymer is injected with high velocity/pressure into a thin mold. The mold is cooled during the filling processes and the following packing stage. The product is ejected from the mold as soon as the polymer has completely solidified. Normally the whole production process takes a couple of seconds [6, 9].

Mathematical modeling is an important tool for the analysis and the prediction of the product's physical properties. The complete model for injection molding process involves mass, momentum and energy balance equations, combined with constitutive laws for non-Newtonian fluids. The locations of the advancing fluid

¹kemelli@icmc.usp.br, Ph.D. student financially supported by FAPESP grant 05/51040-6

²gnonato@icmc.usp.br, CNPq grant 308292/2006-5

³norberto@uerj.br, CNPq grants 307230/2006-6, 486153/2006-1 and PROCÍENCIA-UERJ

front (free surface) must be determined as part of solution. Since products are very thin, a Hele-Shaw type approximation can be used for the flow. This simplifies the momentum balance equation dramatically and results in a 2D flow problem. The heat transfer problems is, nevertheless, 3D. For this reason this approach is called $2^{1/2}$ D [10, 13]. In the present work we shall, however, solve the differential equations considering Newtonian and isothermal fluid flows.

The purpose of the present contribution is to formulate and evaluate a meshless simulation framework for the filling stage of injection molding process, where no mesh is applied for the set of field variables, such as mass, momentum, energy, position, etc. Meshless methods use a finite number of scattered particles, also denominated nodes or points, within the problem domain and on the boundaries of the domain to represent – not discretize – the problem domain, its boundaries and such flow variables [1, 4, 11]. The discretization method applied for approximate the flow variables is based on an Eulerian frame of the Smoothed Particle Hydrodynamics (SPH) formulation [7, 12]. The governing equation for free-surface position is solved based on a meshless adaptation of Volume of Fluid Method [8].

2. The Governing Equations

The 3D conservation equations, governing the motion of an isothermal fluid flow, can be written as follow

Continuity Equation

$$\frac{\partial \rho}{\partial t} + \nabla \cdot \rho \mathbf{v} = 0. \quad (2.1)$$

Momentum Equation

$$\frac{\partial}{\partial t}(\rho \mathbf{v}) = \rho \mathbf{g} + \nabla \cdot \underline{\sigma} - \nabla \cdot \rho \mathbf{v} \mathbf{v}. \quad (2.2)$$

where ρ is the fluid density, t is time, $\mathbf{v} = (v_x, v_y, v_z)$ is the fluid velocity, \mathbf{g} is the total body force per unit mass and $\underline{\sigma}$ is the stress tensor. These equations are quite general and hold for common fluids. However, even with current computers, solving them in complicated domains as injection molds with cavities is considered a very difficult task. Consistently with most injection mold applications some simplifications can be applied over those governing equations, regarding the following assumptions

- i. During the filling phase, the fluid is considered to be incompressible;
- ii. The fluid is considered a Generalized Newtonian Fluid;
- iii. Simplification by dimensional analysis: the idea is to obtain estimates for the order of magnitude of each term in the governing equations – terms of sufficiently low order have little influence and, therefore, can be neglected. This analysis is made using characteristic values of the variables [10].
- iv. Simplification by mathematical analysis: since the molds are represented by weakly curved surfaces, local coordinate systems restricted to the surfaces

can be defined providing 2D manipulations and allowing integration of momentum and continuity equations across the thickness. The resulting equation is called Hele-Shaw equation

$$\nabla \cdot (S_2 \nabla p) = 0, \quad (2.3)$$

where p is the pressure and the quantity S_2 is called fluidity. For symmetrical molds S_2 is defined by

$$S_2 = \int_0^h \frac{z'^2}{\eta} dz',$$

where h is the mold thickness and η is the viscosity of the fluid.

In injection molding process the fluid is usually modeled as a Generalized Newtonian fluid, however, in this work we assume that the fluid is Newtonian. This assumption allows extra simplifications in both fluidity and velocity field

$$S_2 = \frac{h^3}{3\eta}, \quad v_x = \frac{1}{2\eta} \frac{\partial p}{\partial x} (z+h)(z-h) \quad \text{and} \quad v_y = \frac{1}{2\eta} \frac{\partial p}{\partial y} (z+h)(z-h).$$

where z is the current mold layer where the velocities are computed and for symmetrical molds, $0 \leq z \leq h$. Finally, Eq. (2.3) should be solved subject to the following boundary conditions: *i*) the pressure is zero on the free surface; *ii*) the pressure or the flow rate is defined in the inlet regions and *iii*) the pressure gradient in the normal direction is zero in any impermeable boundary.

The numerical solution of the governing equation for the filling phase with a Newtonian fluid is made in two main stages: calculation of the pressure field and the free surface motion [10]. In our method, the pressure equation is solved by an Eulerian approach based on Smoothed Particle Hydrodynamics Method. The prediction of the free surface position is obtained by a meshless Volume of Fluid Method. It is important to notice that the literature does not present a similar approach as the one described in the following section.

3. Solution of Pressure Equation

The Smoothed Particle Hydrodynamics (SPH) theory is based on integral representation of functions and it was developed by Lucy [12] and Gingold and Monaghan [7]. The SPH creators noticed that any function f , defined over a domain of interest and representing some physical variable, can be expressed in terms of its values at a discrete set of disordered points (SPH particle positions) by suitable definition of a specially smoothing kernel (weight) function with compact support. Therefore, the partial differential equations describing the conservation laws can be transformed into corresponding integral form using this approach.

Given a function f defined over the entire domain Ω , we can always write

$$f(\mathbf{x}) = \int_{\Omega} f(\mathbf{x}') \delta(\mathbf{x} - \mathbf{x}') d\mathbf{x}',$$

where $\delta(\mathbf{x})$ is the 3D Dirac delta distribution. Since the Dirac delta is not a function, it should be replaced with an interpolating kernel $W(\mathbf{x}, r)$, resulting in

$$\langle f(\mathbf{x}) \rangle = \int_{\Omega} f(\mathbf{x}') W(\mathbf{x} - \mathbf{x}', r) d\mathbf{x}',$$

which clearly represents an approximation for $f(\mathbf{x})$, since the kernel does not exactly substitute the Dirac delta. Next, the interpolant integral can be replaced by

$$\langle f(\mathbf{x}) \rangle \approx \sum_b m_b \frac{f_b}{\rho_b} W(\mathbf{x} - \mathbf{x}_b, r),$$

where the summation index b denotes the particle labels, and the summation is over all elements. Particle b has mass m_b , position \mathbf{x}_b , density ρ_b and velocity \mathbf{v}_b , $f(\mathbf{x}_b)$ is denoted as f_b and r is the support radius. Since the Eulerian reference frame is used, the particle density and mass are constants, and are incorporated in W .

The finite integral representation is valid and converges when the weight function satisfies certain conditions [1, 4]

$$W(\mathbf{x}, r) > 0 \text{ on a subdomain of } \Omega, \Omega_I,$$

$$W(\mathbf{x}, r) = 0 \text{ outside the subdomain } \Omega_I,$$

$$\int_{\Omega} W(\mathbf{x}, r) d\Omega = 1 \text{ normality property,}$$

$$W(\mathbf{x}, r) \text{ is a monotonically decreasing function,}$$

$$W(\mathbf{x}, r) \rightarrow \delta(\mathbf{x}) \text{ as } r \rightarrow 0.$$

Three weight functions commonly used are the exponential, the cubic spline and the quartic spline. They are illustrated in Fig. 1.

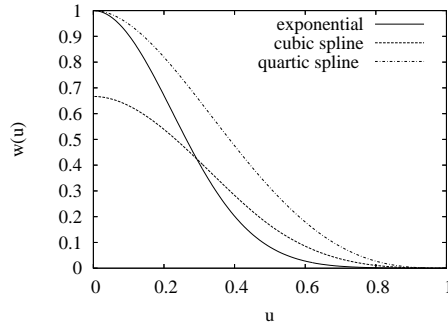


Figure 1: Three commonly used weight functions: exponential, cubic spline and quartic spline.

In this work, we employ the exponential function

$$w(u) = \begin{cases} e^{-\frac{u^2}{\alpha}} & \text{if } u \leq 1 \\ 0 & \text{if } u > 1 \end{cases}, \quad (3.1)$$

where α is a constant commonly taken as $\alpha = 0.3$ [11] and the argument of $w(u)$ is $u = \|\mathbf{x} - \mathbf{x}'\|/r$, where r is the support radius.

A differentiable interpolant of a function can be constructed from its values at the particles (interpolation points) by using a differentiable kernel. Consequently, the derivatives of this interpolant are obtained by ordinary differentiation of the kernel function. Therefore, the SPH approximation of Eq. (2.3) is given by

$$\sum_b p_b \nabla \cdot (S_2 \nabla w(\mathbf{x} - \mathbf{x}_b, r)) = 0. \tag{3.2}$$

Eq. (3.2) can be expressed as a linear system, $Lp = f$, where L is the coefficient matrix, p is a vector with unknown values of pressure and f is a vector associated to the boundary conditions. Matrix L is sparse and symmetric, thus the resulting linear system can be solved using efficient computational methods, such as the Conjugate Gradients Method with Incomplete Cholesky Pre-Conditioner. Moreover, the dimension of matrix L is of the order of number of particles. Each diagonal element is associated with a particle *part*, and the non zeros elements of the matrix row are associated with the nearest neighbors to particle *part*, according to Eq. (3.1) for the support radius.

4. Moving the Free Surface

In order to identify and advance the free surface of the fluid, a Meshless adaptation of Volume of Fluid technique (VOF) is used [8]. The main idea in VOF method is to introduce a function ϕ whose average value represents the fractional volume of the cell occupied by the fluid. This filling factor ranges in the interval $[0, 1]$: if ϕ of a particle is equal to 1, this means that the control volume associated with that particle is completely full of fluid and if ϕ of the particle is equal to 0, then the control volume associated with the particle is completely empty. Intermediate values of ϕ indicate that the control volume is partially full, evidencing the free surface position. The time dependence of ϕ is governed by a pure advection equation whose integral form is

$$\int_V \left(\frac{\partial \phi}{\partial t} + \nabla \cdot (\mathbf{v} \phi) \right) dV = 0. \tag{4.1}$$

In case of meshless methods there are no cells, elements or control volumes, so it is necessary to associate a fictitious volume to each discretization particle, as the one illustrated in Figure 2.

Applying Gauss Theorem, Eq. (4.1) turns to be

$$\frac{\partial}{\partial t} \int_V \phi dV + \int_S \phi \mathbf{v} \cdot \mathbf{n} dS = 0,$$

where V is the “meshless volume” and S is the “meshless boundary” of V .

Related to finite volume V_i , the rate of volume of the fluid in particle i (abbreviated by *part_i*) is equal to the sum of the contributions proceeding from neighboring

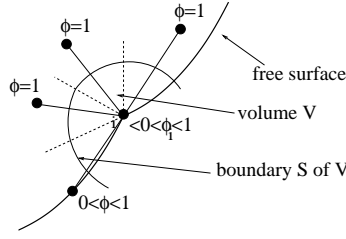


Figure 2: “Meshless” volume V and boundary S of V associated to particle i .

particles j where $\phi(\text{part}_j) = 1$. Furthermore, considering that ϕ is uniform inside the volume of part_i , it is possible to approximate the above equations as

$$V_i \frac{\partial \phi(\text{part}_i)}{\partial t} = - \int_S \phi(\text{part}_j) \mathbf{v} \cdot \mathbf{n} dS,$$

where the surface integral includes the contribution of all volumes associated to full particles, $\phi(\text{part}_j) = 1$. Therefore, approximating the time derivative using finite differences, we have

$$\phi(\text{part}_i)^{n+1} = \phi(\text{part}_i)^n - \frac{\Delta t}{V_i} \int_S \phi(\text{part}_j) \mathbf{v} \cdot \mathbf{n} dS. \quad (4.2)$$

where Δt is the time-step and index n is related to time discretization.

The term $\mathbf{v} \cdot \mathbf{n}$ is the velocity in ji -direction, i.e.,

$$\mathbf{v} \cdot \mathbf{n} = -k \frac{p_j - p_i}{\|\mathbf{x}_j - \mathbf{x}_i\|},$$

where $k = S_2/h$. Considering an isotropic random distribution of particles, we define the average radius, volume and area for particle i , respectively, as

$$R_i = \frac{1}{n_p} \sum_{j=1}^{n_p} \|\mathbf{x}_j - \mathbf{x}_i\|, \quad V_i = \pi R_i^2 \quad \text{and} \quad A_{ij} = 2\pi R_i.$$

where n_p is the number of particles in the neighborhood of particle i . Finally substituting these values on Eq. (4.2), the resulting equation for the filling factor, ϕ , associated to particle i is obtained

$$\phi(\text{part}_i)^{n+1} = \phi(\text{part}_i)^n + \frac{2\Delta t}{R_i} \sum_j k_{ij} \frac{p_j - p_i}{\|\mathbf{x}_j - \mathbf{x}_i\|}, \quad (4.3)$$

where k_{ij} is an average value, given by

$$k_{ij} = \begin{cases} \frac{2}{\frac{h_i}{S_{2_i}} + \frac{h_j}{S_{2_j}}} & \text{if } \phi(\text{part}_j) = 1 \\ 0 & \text{if } \phi(\text{part}_j) \neq 1 \end{cases}$$

The harmonic mean is preferable over the arithmetic mean because it produces the exact solution in case of a sharp variation of S_2/h located half way between particles i and j .

After computation of the ϕ factor variation in time for all particles, it is possible to calculate the time step, Δt_{fill_i} , that is necessary to accurately fill the control volume associated with particle i where $0 \leq \phi \leq 1$. For that purpose, $\phi(part_i)^{n+1} = 1$ is imposed on Eq. (4.3) therefore providing an expression for Δt_{fill}

$$\Delta t_{fill} = \frac{R_i(1 - \phi(part_i)^n)}{\sum_j k_{ij} \frac{p_j - p_i}{\|\mathbf{x}_j - \mathbf{x}_i\|}}$$

At each time step, the time interval is chosen such that only one control volume is filled, or, in other words, the time step is calculated for all non-filled particles and the smallest one is chosen for advancement of the free-surface. This strategy results in a scheme with low numerical diffusion.

5. Results

The implemented numerical method has been validated considering constant thickness and fluidity with Dirichlet and Neumann boundary conditions, against both analytical and numerical solution obtained by Finite Volume Method (FVM) [5]. In this section, we present some results of numerical solution of equations (2.3) and (4.1) for general situations. In these simulations, we use prescribed pressure at the mold inlet, as $p = 10^5 \text{ N/m}^2$, and the mold thickness is $h = 10^{-2} \text{ m}$.

In the first simulation we present a comparison between results obtained through FVM and the implemented one during the filling of a key-shaped mold with one circular insertion. Figure 3 shows the mold dimensions, the unstructured triangular mesh used in FVM and the scattered points used in our method, respectively.

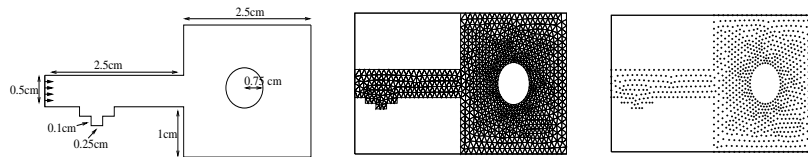


Figure 3: Dimensions of the complex key-shaped mold, unstructured mesh used in FVM and scattered points for implemented method.

The unstructured triangular mesh was built by a free 2D quality mesh generator based on Delaunay triangulation called Easymesh [3] and has 1713 elements and 942 control volumes. Only these 942 points defining the control volumes were used in the presented approach.

Figure 4 shows the pressure and velocity vector, respectively. The snapshots represent the fluid flow during the mold filling at 6.45, 21.95 and 39.81 seconds. The predicted injection time is 39.82 seconds. Notice that the results obtained through both methods are quite similar.

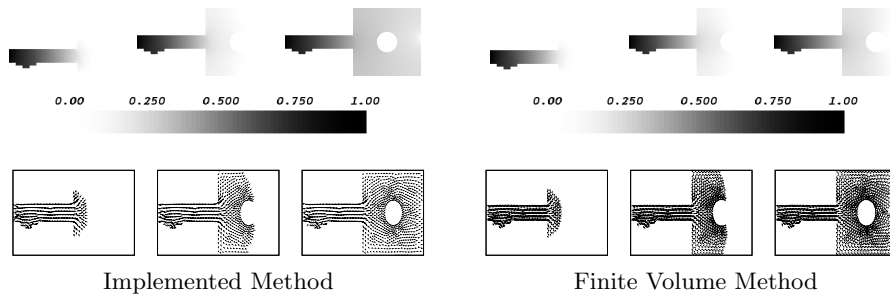


Figure 4: Three stages of pressure distribution and velocity field during mold filling. The values of pressure are scaled by $p_0 = 10^5 N/m^2$.

In the second simulation, a mold of Tweety Bird was filled aiming to illustrate the capability of the presented method to deal with complex non planar geometries. The scattered points representing the Tweety Bird are 3D and they range of $0.2355 m$ in x -direction, $0.3675 m$ in y -direction and $0.0180 m$ in z -direction, as illustrated in Figure 5. In this case, the inlet region is the biggest hair of Tweety Bird.

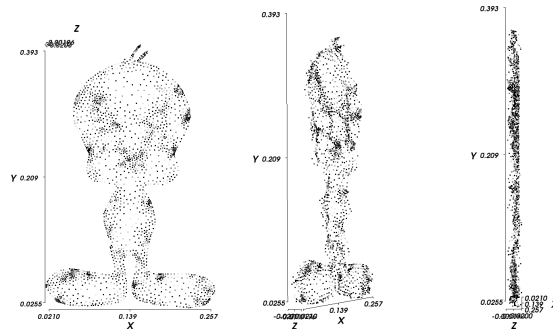


Figure 5: Three views of point set surface defining Tweety Bird's mold.

Figures 6 and 7 show the pressure and velocity fields, respectively, at five stages: right after the flow had started, at three intermediate times and at its end. The total predicted filling time is 0.12 seconds. Although the implemented numerical method avoids completely the use of meshes, a 3D mesh was built with *iMesh*, a quality mesh generator from images [2], aiming depict the pressure field.

6. Conclusion

This work presented a meshless framework for solving the governing equations of fluid flow during the filling phase of injection molding based on adaptations of SPH and VOF methods. For the pressure field an Eulerian approach of SPH method was employed and for predicting the free surface position a meshless scheme of VOF method, considering meshless areas and volumes, also was deduced. This methodology allows to simulate complex geometries, in $2^{1/2}D$, without excessive computational efforts, regarding specially to mesh generation/maintenance. Therefore, this

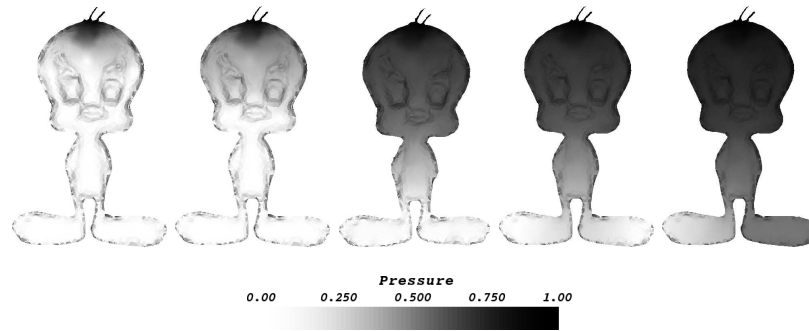


Figure 6: Five stages of pressure distribution during mold filling. The values are scaled by $p_0 = 10^5 N/m^2$.

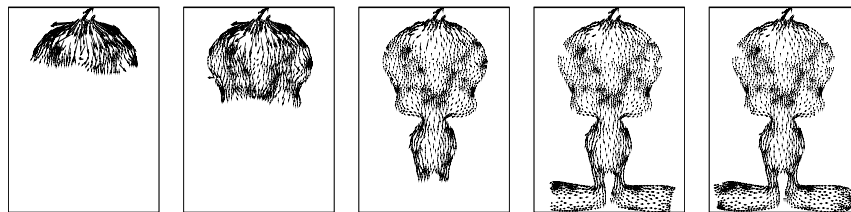


Figure 7: Five stages of velocity field.

work may be considered an useful tool for the design, analysis and troubleshooting of injection molding process, which is sufficiently accurate for most applications.

Resumo. Neste trabalho uma técnica *meshless* para a simulação do preenchimento de moldes é apresentada. A equação governante para este tipo de problema é nomeada Hele-Shaw e obtida por meio de algumas simplificações nas equações de conservação 3D. Esta aproximação é também chamada $2^{1/2}D$, referindo-se às limitações da geometria do molde como sendo estreito e pouco curvado. Como produtos manufaturados por moldagem por injeção na vida real, como por exemplo baldes, pára-choques de automóveis e carcaças de telefones celulares, não são planares, neste trabalho a cavidade do molde é modelada por superfícies definidas por pontos. Desta forma, nenhum esforço computacional relacionado à geração e à manutenção de malhas é requerido para a solução numérica das equações governantes do escoamento. A técnica desenvolvida para simular a posição da superfície livre, o campo de velocidades e a distribuição de pressão em processos de moldagem por injeção usando-se esta aproximação $2^{1/2}D$ é apresentada e discutida. Os detalhes de nossa aproximação, que é baseada nos métodos *Smoothed Particle Hydrodynamics* e *Meshless Volume of Fluid*, também são apresentados.

References

- [1] T. Belytschko, Y. Krongauz, D. Organ, M. Fleming, P Krysl. Meshless methods: An overview and recent developments, *Comput. Methods Appl. Mech. Engrg.*, **139** (1996), 3–47.

- [2] A.J. Cuadros-Vargas, L.G. Nonato, Imesh: Quality mesh generation from images in “ECCOMAS - European Congress On Computational Methods in Applied Sciences and Engineering”, 2006, Egmond aan Zee, Netherlands.
- [3] Easymesh: a free 2D quality mesh generator based on Delaunay triangulation. <http://www-dinma.univ.trieste.it/nirftc/research/easymesh/> [05 July 2007].
- [4] M. Ellero, R.I. Tanner, SPH Simulations of Transient Viscoelastic Flows at Low Reynolds Number, *Journal of Non-Newtonian Fluid Mechanics*, **132**, No. 1-3 (2005), 61–72.
- [5] K.C. Estacio, L.G. Nonato, N. Mangiavacchi, Solution of Hele-Shaw Equation in Surfaces Defined by Non Organized Points, in “XXVII CILAMCE - Iberian Latin American Congress on Computational Methods in Engineering”, 2006, Belém, Brazil.
- [6] K.C. Estacio, N. Mangiavacchi, Simplified model for mold filling simulations using CVFEM and unstructured meshes, *Communications in Numerical Methods in Engineering*, **23**, No. 5 (2007), 345–361.
- [7] R.A. Gingold, J.J. Monaghan, Smoothed particle hydrodynamics: theory and application to non-spherical stars, *Mon. Roy. Astron. Soc.*, **181** (1977), 375–389.
- [8] C.W. Hirt, B.D. Nichols, Volume of fluid (VOF) method for the dynamics of free boundaries, *Journal of Computational Physics*, **39** (1981), 201–225.
- [9] E. Holm, H. Langtangen, A unified finite element model for the injection molding process, *Computer Methods in Applied Mechanics and Engineering*, **178** (1999), 413–429.
- [10] P. Kennedy, “Flow Analysis of Injection Molds”, Hanser Publishers, New York, 1995.
- [11] G.R. Liu, “Meshfree Methods – Moving Beyond the Finite Element Method”, CRC Press, 2003.
- [12] N.B. Lucy, A numerical approach to the testing of frission, *Astronomical Journal*, **82** (1977), 1013–1024.
- [13] C.L. Tucker III, editor, “Computer Modeling for Polymer Processing - Fundamentals”, Computed Aided Engineering for Polymer Processing. Hanser Publishers, Munich, 1989.